Supporting Information

Ultrafast Fenton-like reaction route to FeOOH/NiFe-LDH heterojunction electrode for efficient oxygen evolution reaction

Yan Liang [a], Jun Wang [a],*, Depei Liu [b], Lin Wu [a], Taozhu Li [c], Shicheng Yan [c],*, Qi Fan [a,d],*, Kai Zhu [e],*, Zhigang Zou [b,c]

[a] Key Laboratory of Solar Energy Science and Technology in Jiangsu Province, Southeast University, No. 2 Si Pai Lou, Nanjing, Jiangsu 210096, P. R. China, E-mail: 101010980@seu.edu.cn

[b] National Laboratory of Solid State Microstructures, Jiangsu Key Laboratory for Nano Technology, School of Physics, Nanjing University, No. 22 Hankou Road, Nanjing, Jiangsu 210093, P. R. China

[c] Jiangsu Key Laboratory for Nano Technology, Jiangsu Key Laboratory of Artificial Functional Materials, Eco-materials and Renewable Energy Research Center (ERERC), Collaborative Innovation Center of Advanced Microstructures, College of Engineering and Applied Sciences, Nanjing University, No. 22 Hankou Road, Nanjing, Jiangsu 210093, P. R. China, E-mail: yscfei@nju.edu.cn

[d] School of Materials Science and Engineering, Southeast University, Jiulonghu Campus, Nanjing, Jiangsu 211189, P. R. China, E-mail: fanqi1984@126.com

[e] School of Information Science and Engineering, Nanjing University Jinling College, No. 8, Xuefu Road, Nanjing, Jiangsu 210089, P. R. China, E-mail: zhukai@jlxy.nju.edu.cn

1. Material synthesis

1.1. Chemicals and materials

Analytical reagents $Fe(NO_3)_3 \cdot 9H_2O$, H_2O_2 (30 wt. %) were purchased from Shanghai Chemical Reagent Co., Ltd (China), IrO_2 was purchased from Shanghai Macklin Biochemical Co., Ltd (China) and were used as received without further purification.

1.2. Preparation of FeOOH/NiFe-LDH electrode

Before reaction, a piece of Ni foam was cleaned in 6 M HCl, ethanol, and deionized water with the assistance of ultrasonication each for 10 min. The solution was prepared by dissolving $Fe(NO_3)_3 \cdot 9H_2O$ (1 g) into deionized water (20 mL). Then, the cleaned Ni foam was immersed in the solution. Afterward, drop 30 wt.% H_2O_2 (8 mL) into the above-mentioned solution. After a drastic reaction for 1 min, the sample was taken out and washed with deionized water several times followed by drying at 60 ℃ for 6 h.

1.3. Preparation of NiFe-LDH electrode

To prepare, a piece of Ni foam was cleaned in 6 M HCl, ethanol, and deionized water with the assistance of ultrasonication each for 10 min. Then, $Fe(NO_3)_3 \cdot 9H_2O$ (1 g) was dissolved into deionized water (20 mL). The prepared NF was immersed in the above solution at room temperature for 6 h. Then, the products were obtained and washed with deionized water several times.

1.4. Preparation of IrO_2 electrode

5 mg IrO_2 powder and 30 μL 5 wt.% Nafion solution were dispersed in water (776 μL) and (194 μL) ethanol, and the mixture was ultrasonicated for 30 min to form a homogeneous ink. Then catalyst ink (50 μL) was dropwise loaded onto a Ni foam (1 cm × 1 cm) and dried overnight (mass loading: 0.25 mg cm^{-2}).

2. Characterizations

The field-emission scanning electron microscope (FE-SEM, FEI Nov Nano SEM 230) were used to observe the morphologies and nanostructures of FeOOH/NiFe-LDH, and Transmission electron microscope (TEM, JEM-2100 (HR), Japan) equipped with high-resolution TEM (HRTEM) for morphology and crystal lattice image. The crystalline state and structure were characterized by X-ray diffraction (XRD, Rigaku Ultima III, Japan with CuKα radiation) at 40 kV and 40 mA. X-ray photoelectron spectroscopy (XPS, PHI5000 Versa Probe, ULVAC-PHI, Japan) was used to analyze the element valence state with monochromatized Al Kα excitation. The spectral positions are

corrected by normalizing the C1s spectrum at 284.6 eV and a Shirley background is used for peak fitting. The molar ratio of Ni and Fe was calculated according to the inductively coupled plasma optical emission spectrometer (ICP-OES, PerkinElmer (PE) Optima 5300DV, USA) test result. To detect the formation of ·OH, fluorescence spectroscopy was performed (Fluorolog-3 fluorescence spectrophotometer, USA).

3. Electrochemical measurements

Linear sweep voltammetry (LSV) and cyclic voltammetry (CV) were measured on a CHI 730e electrochemical workstation with a typical three-electrode cell at room temperature. Briefly, the prepared sample was directly used as a working electrode, meanwhile, a standard Ag/AgCl electrode serving as the reference electrode, and a Pt plate serving as the counter electrode. All potentials in this study were given versus reversible hydrogen electrode (RHE) according to the equation of $E(RHE) = E(Ag/AgCl) + 0.0591*pH + 0.197$. The overpotential ($\eta$) was calculated according to the formula of $\eta = E(RHE) - 1.23$ V. The LSV curves were recorded at a scan rate of 1 mV s^{-1} in 1.0 M KOH solution with 90% iR compensation. Electrochemical surface area (ECSA) is measured to determine double-layer capacitance (C_{dl}) values by cyclic voltammetry (CV) method in a scan rate range of 20, 40, 60, 80, and 100 mV s^{-1} in the non-Faradaic region from 0.95 to 1.05 V vs. RHE. ECSA can be calculated by equation $ECSA = C_{dl}/C_s$, where C_s is the specific capacitance of the sample which is usually 0.040 mF cm^{-2} in the alkaline solution. The ECSA-normalized current density is calculated by equation: $j_{ECSA} = j/ECSA$. Electrochemical impedance spectroscopy (EIS) was tested in 1.0 M KOH solution by applying an AC voltage of 10 mV amplitude at the potential of 0.5 V (vs. Ag/AgCl) with frequency from 100 kHz to 0.1 Hz. The stability for OER was tested in the above-mentioned three-electrode cells by the LAND CT3001B battery testing system.
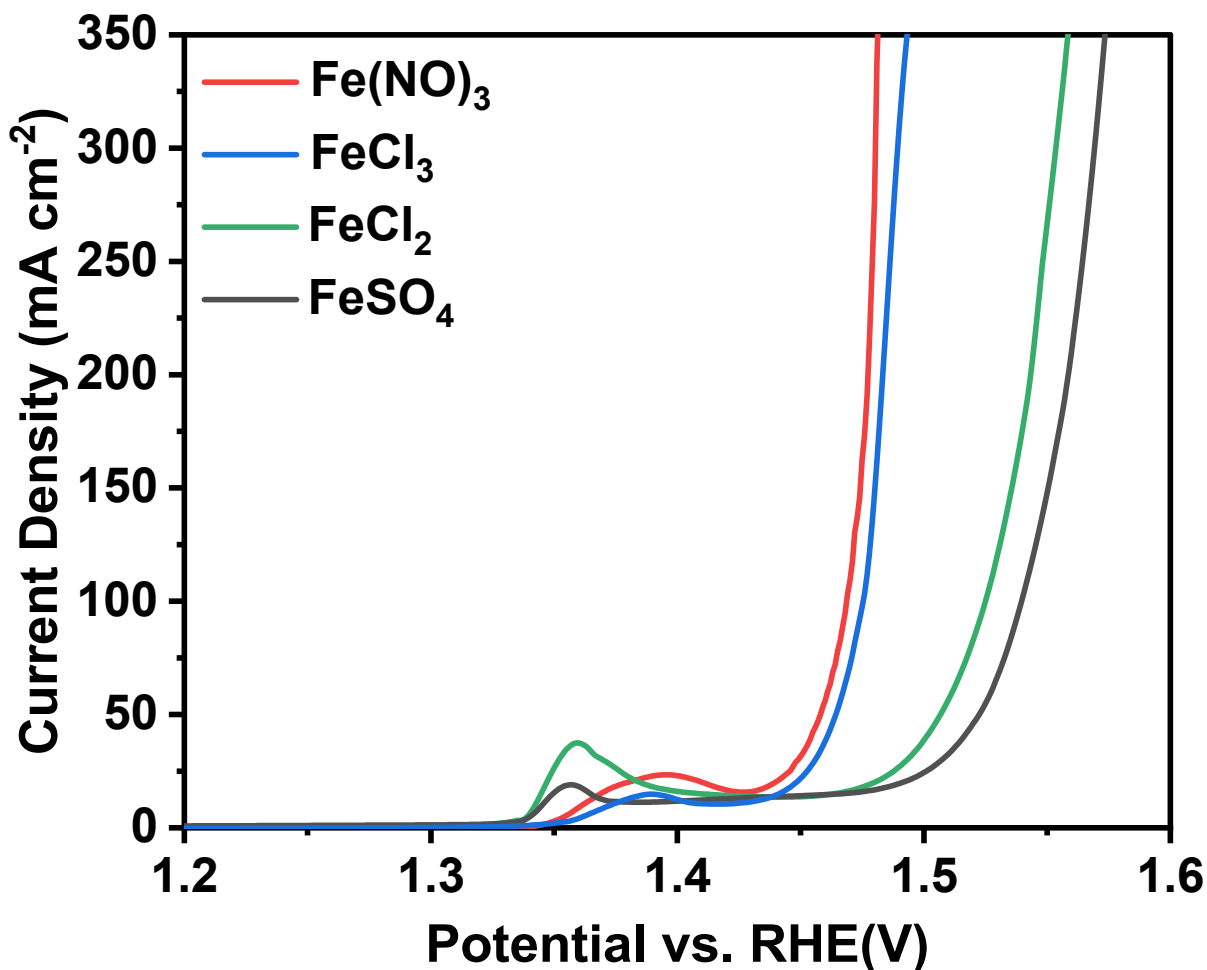
Fig. S1. LSV curves of the samples synthesized by Fenton reagent ($FeCl_2+H_2O_2$ or $FeSO_4+H_2O_2$) or Fenton-like reagent ($FeCl_3+H_2O_2$ or $Fe(NO_3)_3+H_2O_2$). The OER performances of samples obtained by Fenton-like reagent are higher than those of samples obtained by Fenton reagent, nearly did not depend on the anions in Fe-containing precursors. The anions in Fe-containing precursors usually are the insertions of $[Ni^{II}_{1-x}Fe^{III}_x(OH)_2]^{x+}[x\ A^{n/x-}]^{x-}\cdot zH_2O$, A is the inserted anion, which slightly affect the OER activities.

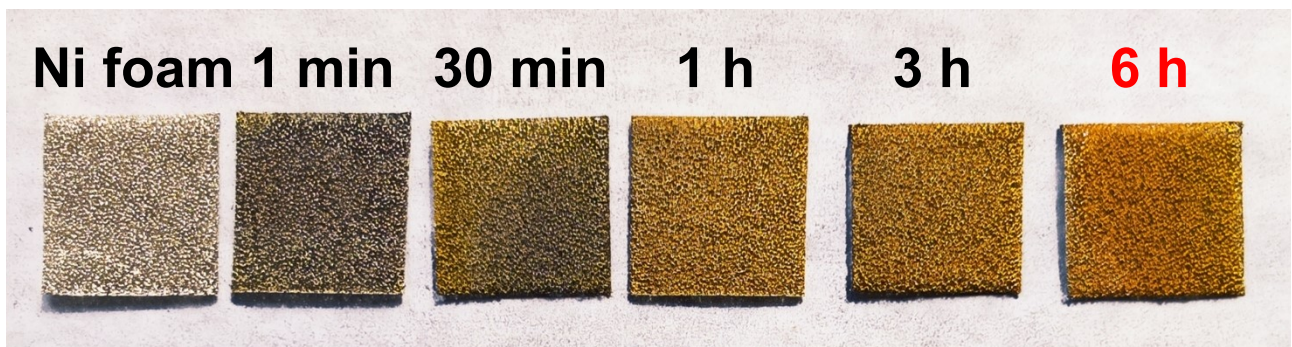**Fig. S2.** Optical photograph to show the formation kinetics of NiFe-LDH by direct reaction of $Fe(NO_3) \cdot _9H_2O$ solution with Ni foam.
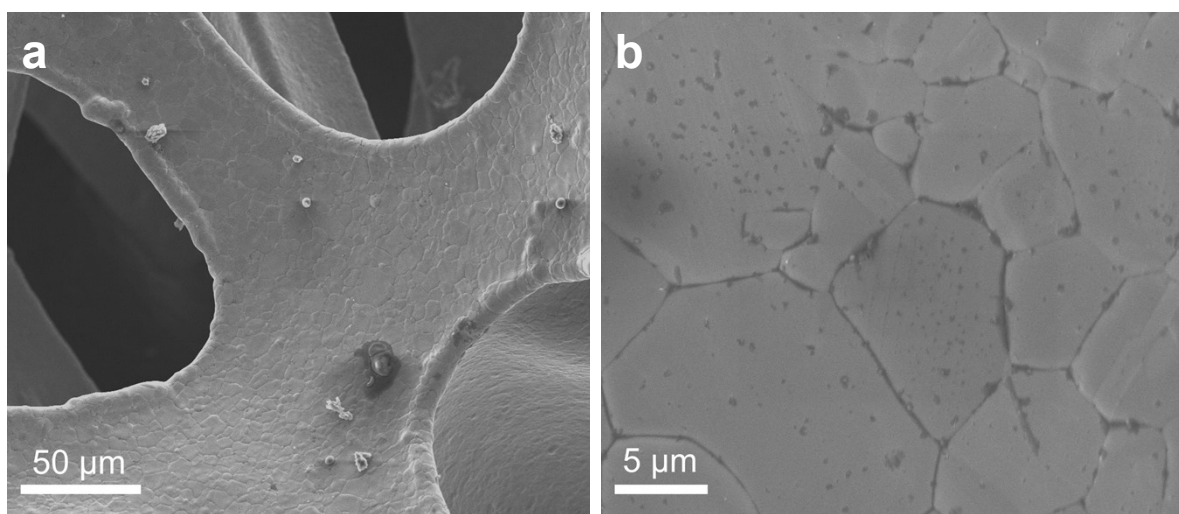
Fig. S3. SEM images of Ni foam 3D skeleton and surface.

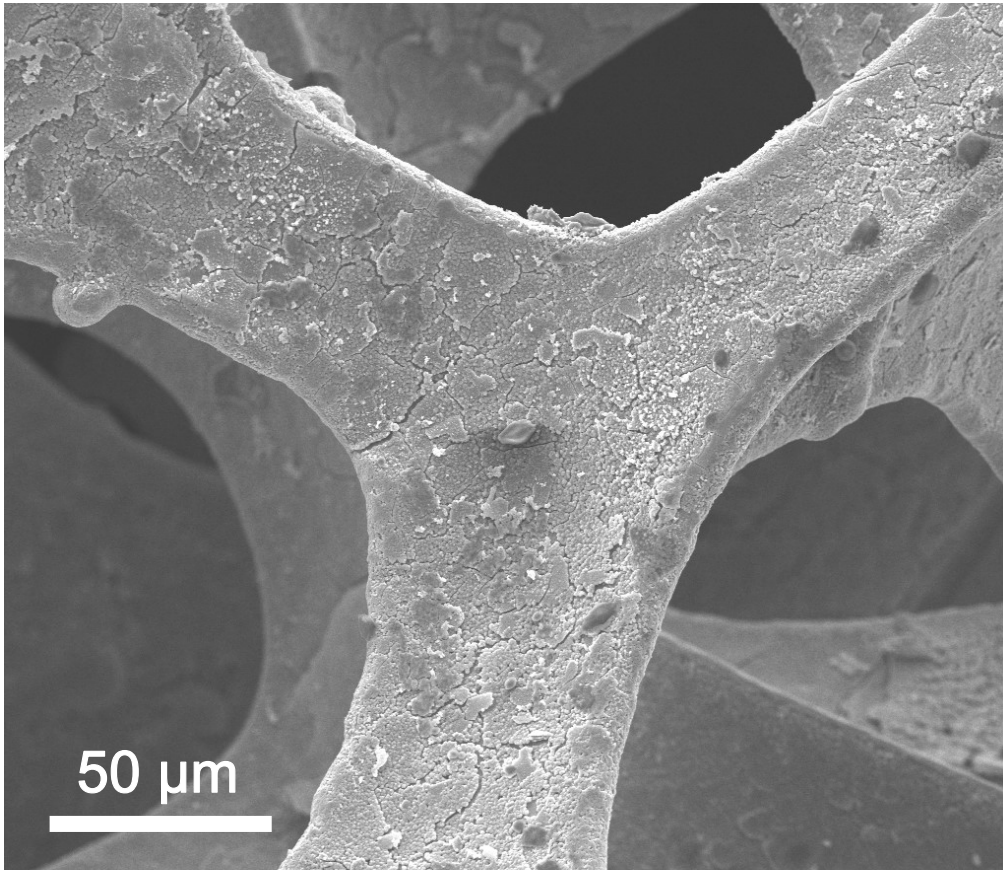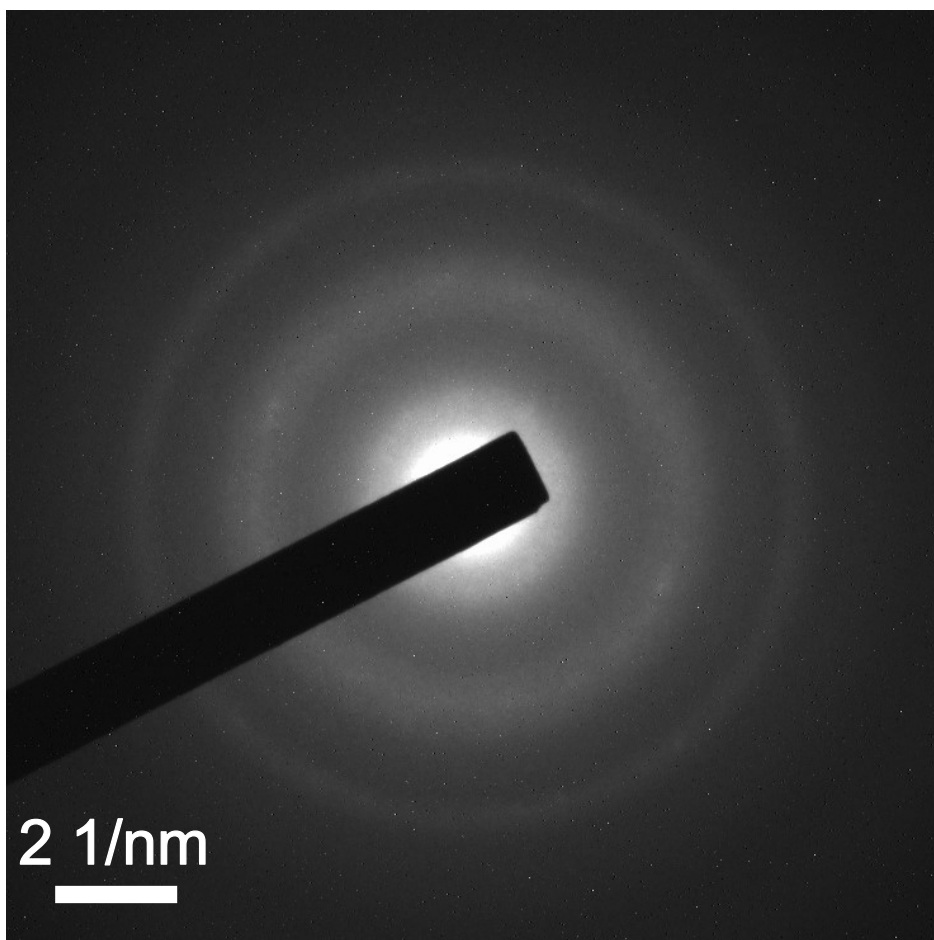**Fig. S4.** SEM images of FeOOH/NiFe-LDH with larger field of view.

Fig. S5. SAED pattern of FeOOH/NiFe-LDH.

CA=117°

Ni foam

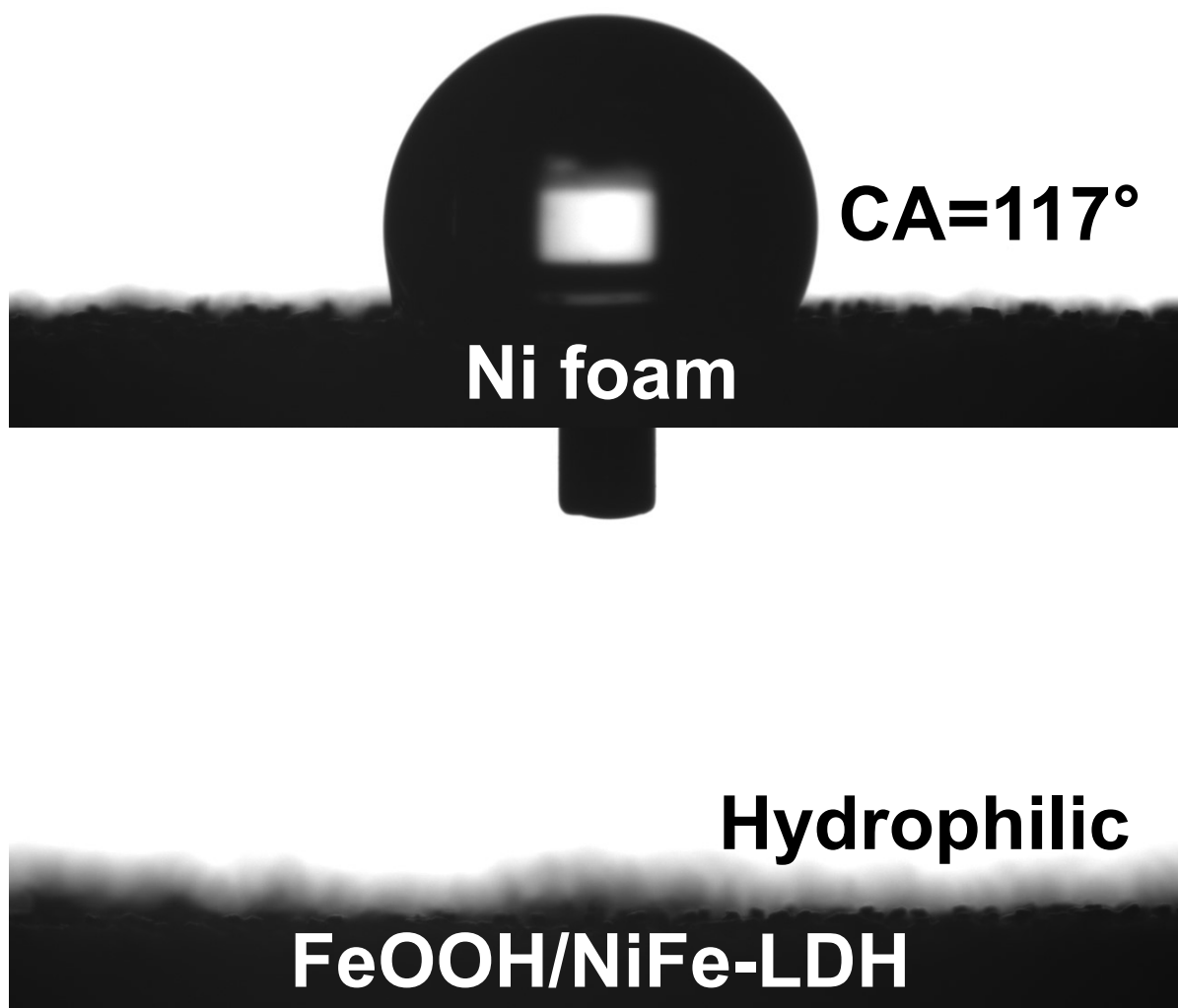Hydrophilic

FeOOH/NiFe-LDH

Fig. S6. Wettability test of Ni foam and FeOOH/NiFe-LDH.
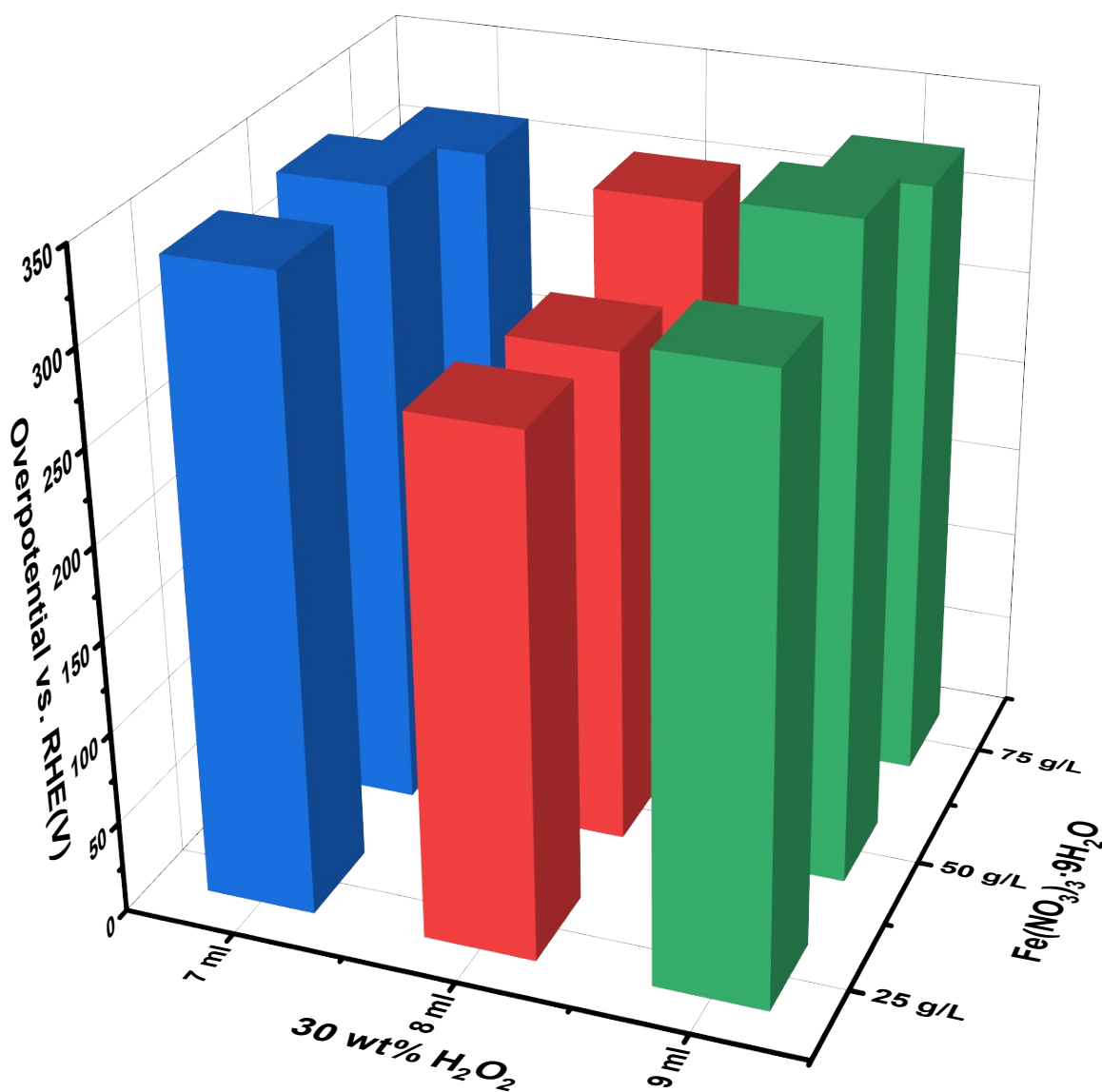
Fig. S7. Overpotentials at 100 mA cm^{-2} of FeOOH/NiFe-LDH based on different usage of H$_2$O$_2$ and Fe(NO$_3$)$_3$·9H$_2$O. The FeOOH/NiFe-LDH with lowest overpotential was obtained by adding H$_2$O$_2$ (8 mL, 30 wt %) into Fe(NO$_3$)$_3$·9H$_2$O solution (50 g L^{-1}, 20 mL). All the Fenton-like reactions are carried out for 1 min.
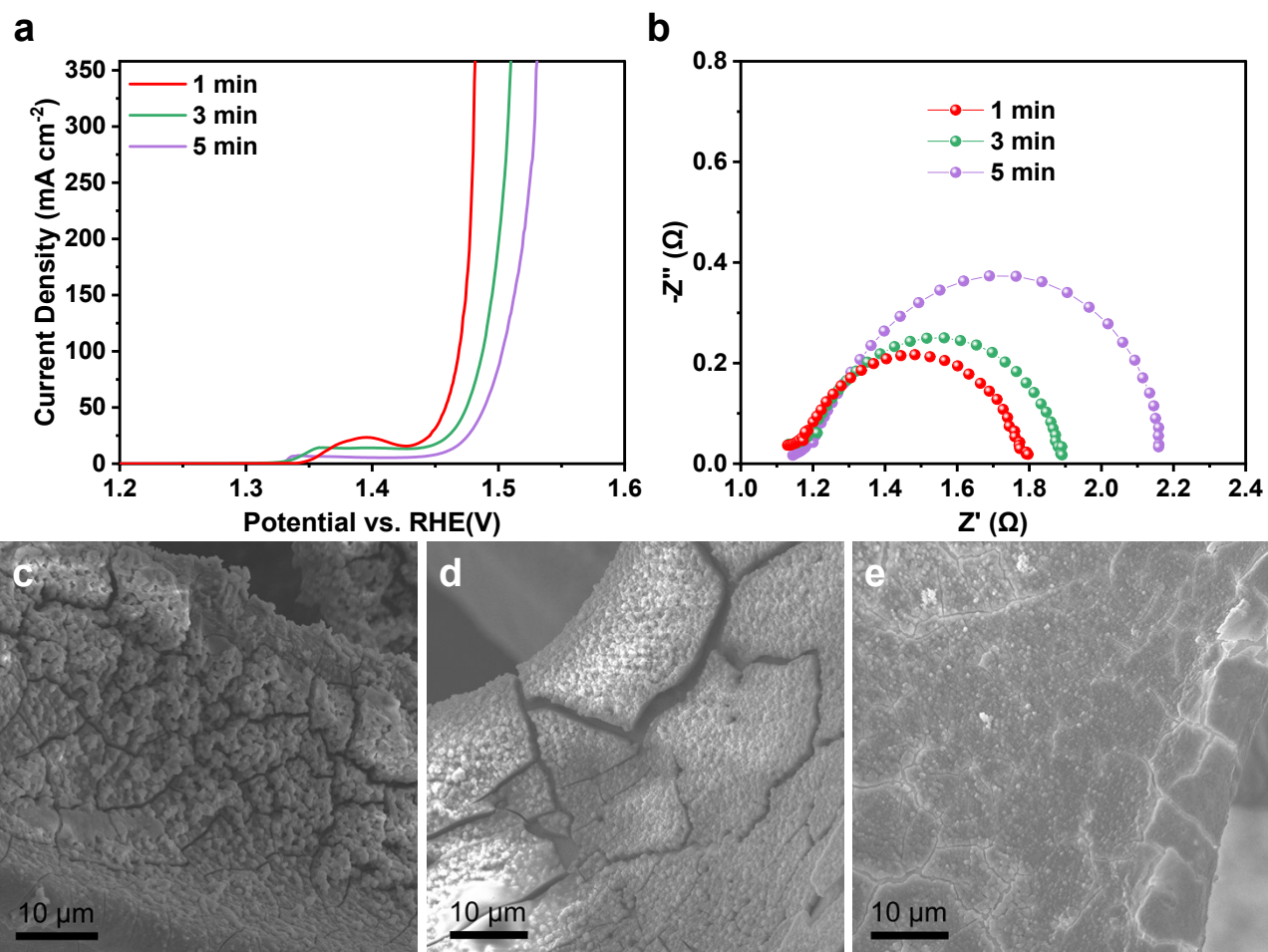
Fig. S8. (a) LSV curves and (b) Nyquist plots of FeOOH/NiFe-LDH based on different reaction time

(c-e) SEM images of FeOOH/NiFe-LDH based on different reaction time (from left to right: 1 min,
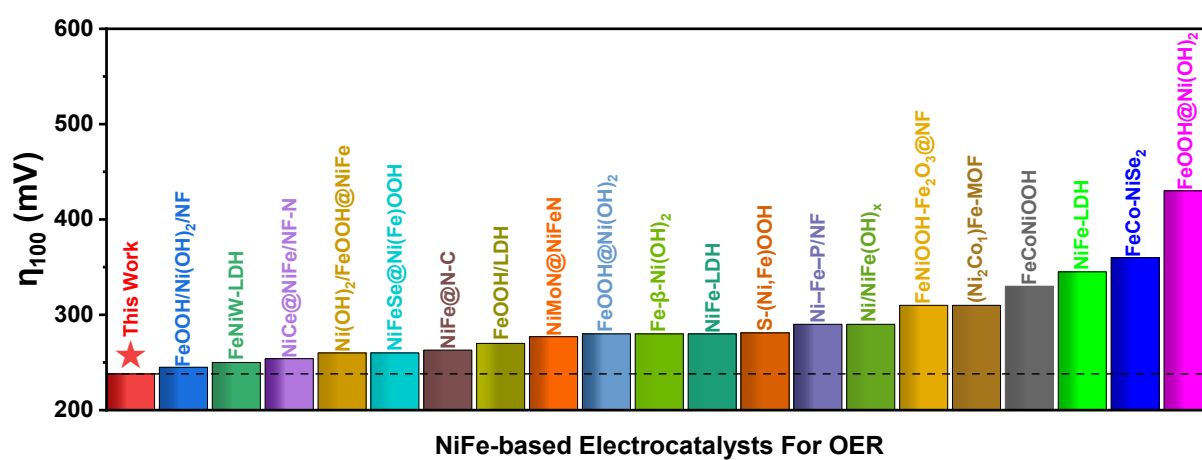
3 min and 5 min).

Fig. S9. The overpotentials (η_{100}, mV) at a current density of 100 mA cm^{-2} for the typical NiFe-based electrocatalysts.
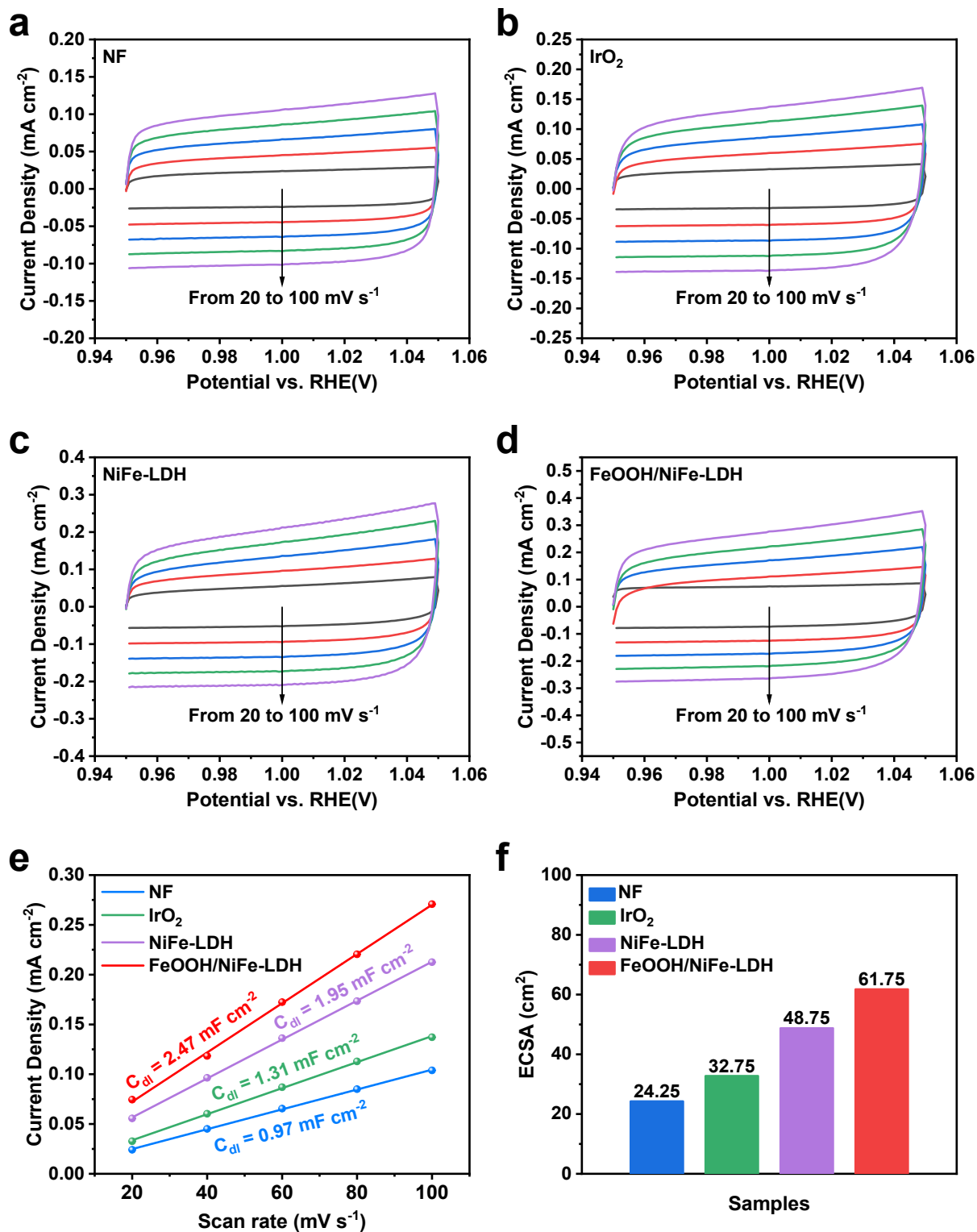
Fig. S10. (a-d) CV curves at scan rates of 20, 40, 60, 80, and 100 mV s^{-1}, (e) calculations of C$_{dl}$ and (f) ECSA for NF, IrO$_2$, NiFe-LDH, and FeOOH/NiFe-LDH electrodes.
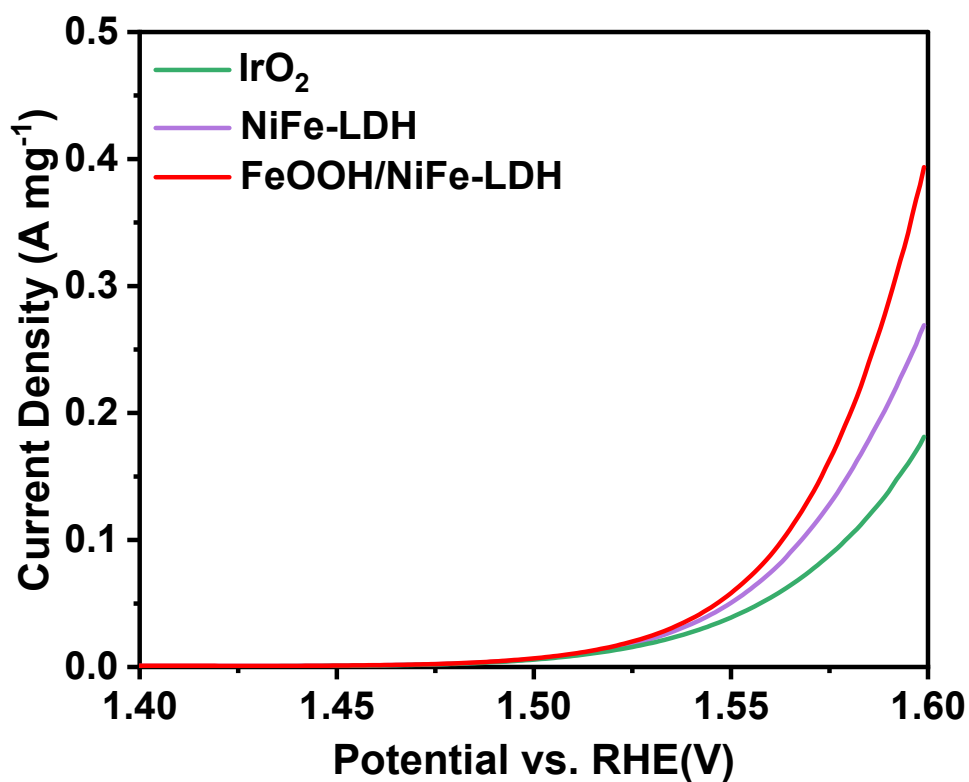
Fig. S11. Mass activity of FeOOH/NiFe-LDH, NiFe-LDH, and IrO$_2$ with the same mass loading (0.25 mg cm^{-2}). The synthesis of FeOOH/NiFe-LDH and NiFe-LDH electrode is the same as IrO$_2$ electrode except the IrO$_2$ powder is replaced by FeOOH/NiFe-LDH and NiFe-LDH.
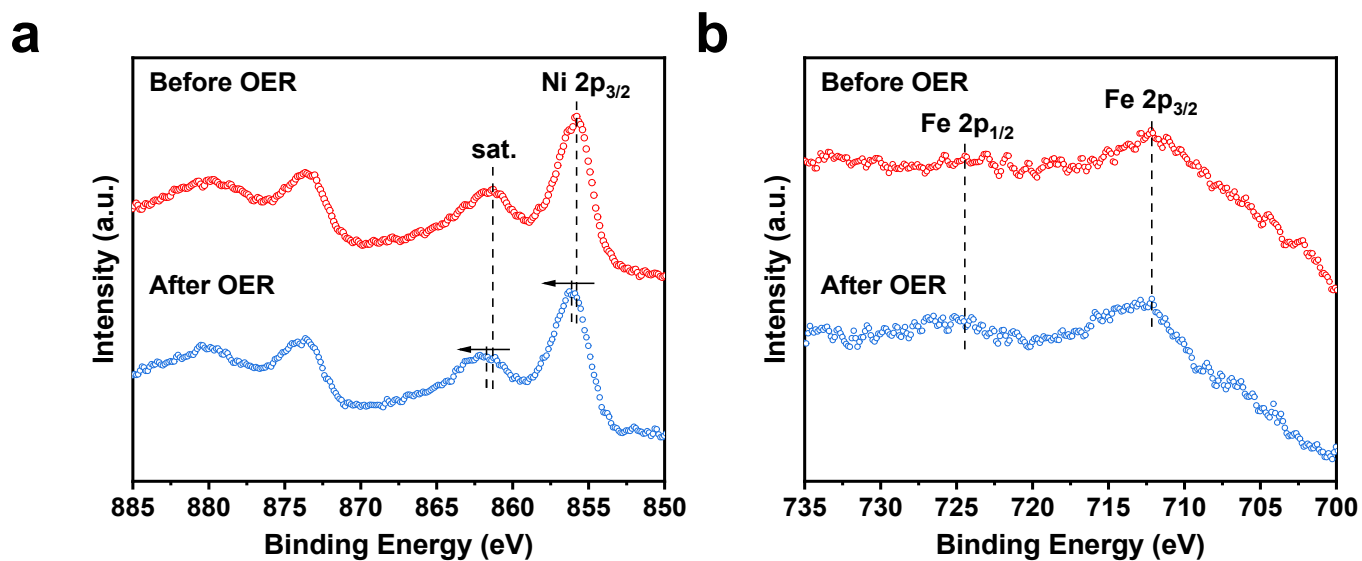
Fig. S12. (a) Ni 2p and (b) Fe 2p XPS spectra of FeOOH/NiFe-LDH before and after long-time OER stability test in 1 M KOH. After the OER test, the peaks of Ni 2p have shifted towards higher binding energy, indicating that Ni^{2+} is oxidized to Ni^{3+} and the formation of NiFeOOH species.
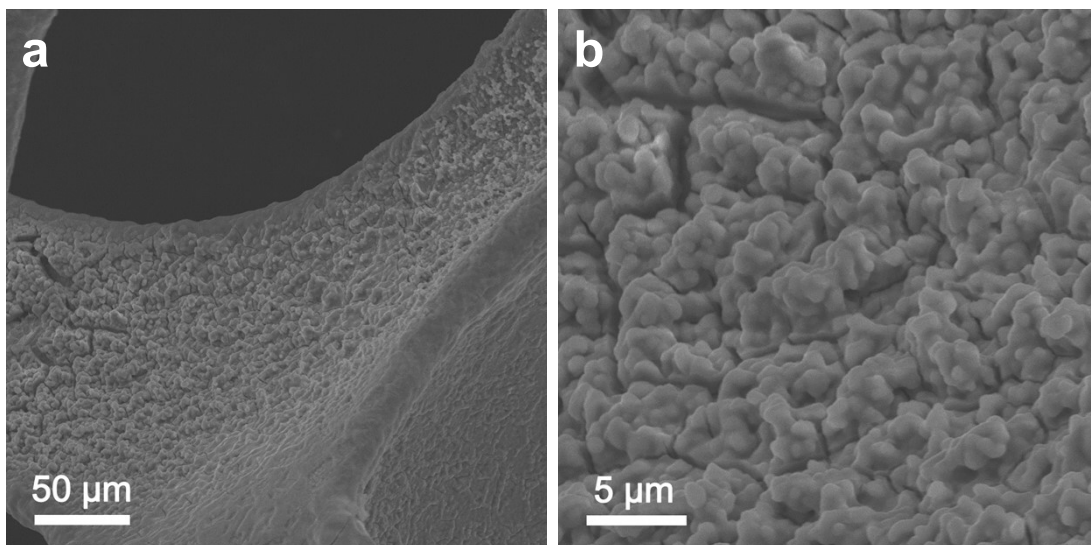
Fig. S13. SEM images of FeOOH/NiFe-LDH after over 700 h OER test.
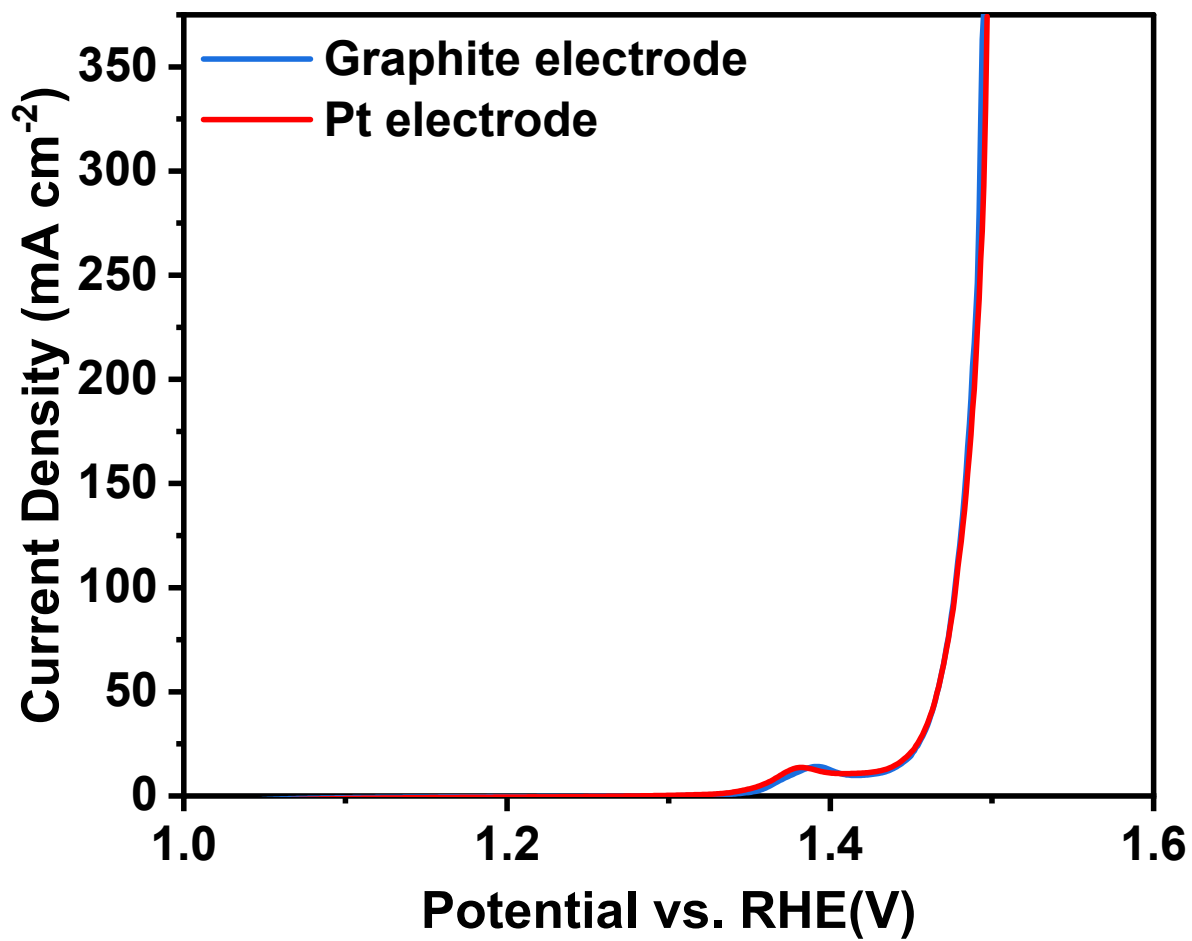
Fig. S14. LSV comparison of FeOOH/NiFe-LDH with counter electrode of Pt and graphite.
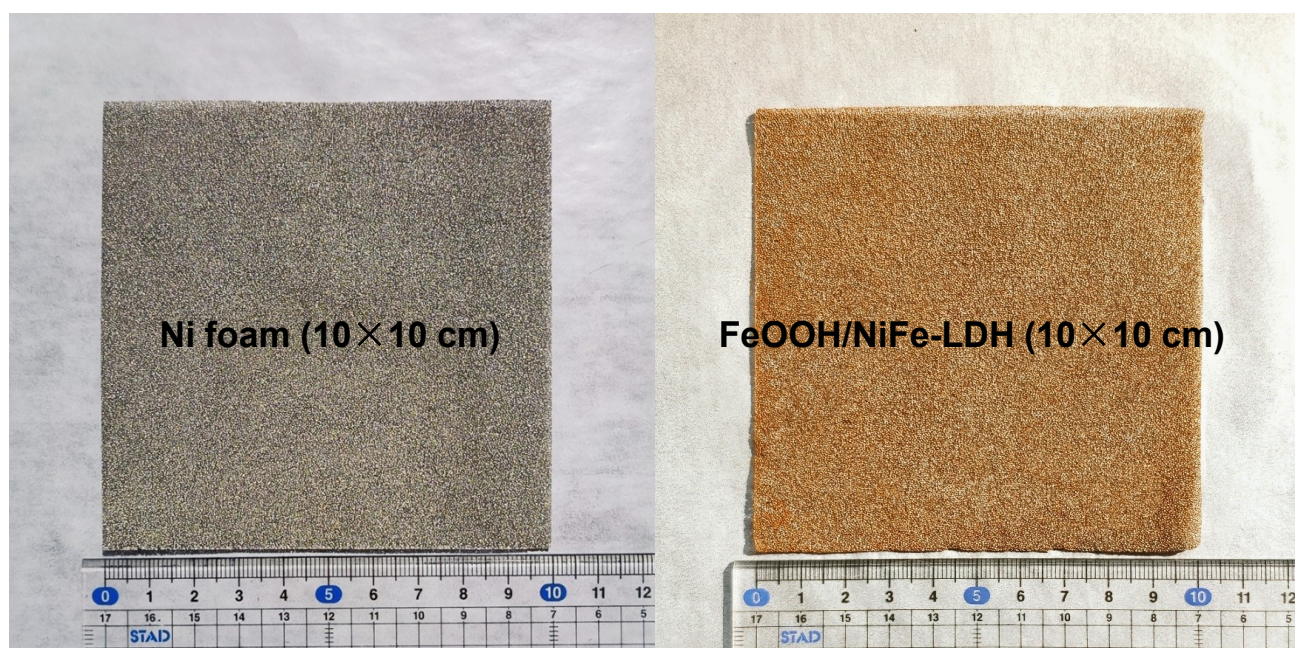
Fig. S15. Optical photographs of Ni foam and FeOOH/NiFe-LDH with large area (10×10 cm).
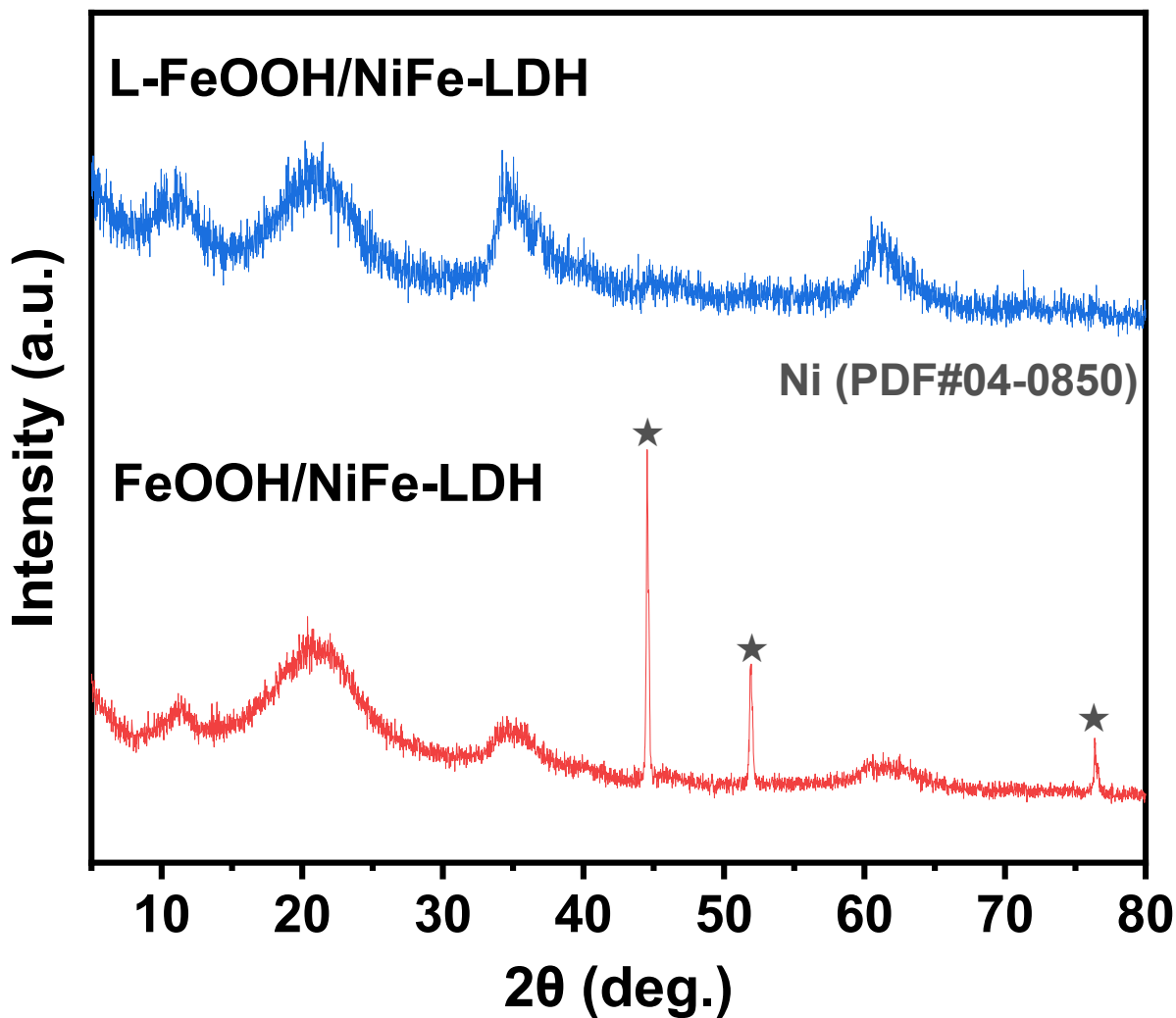
Fig. S16. The XRD pattern of FeOOH/NiFe-LDH and L-FeOOH/NiFe-LDH. The extra three peaks

at 44.5°, 51.8°, and 76.4° of FeOOH/NiFe-LDH are from Ni foam substrate.
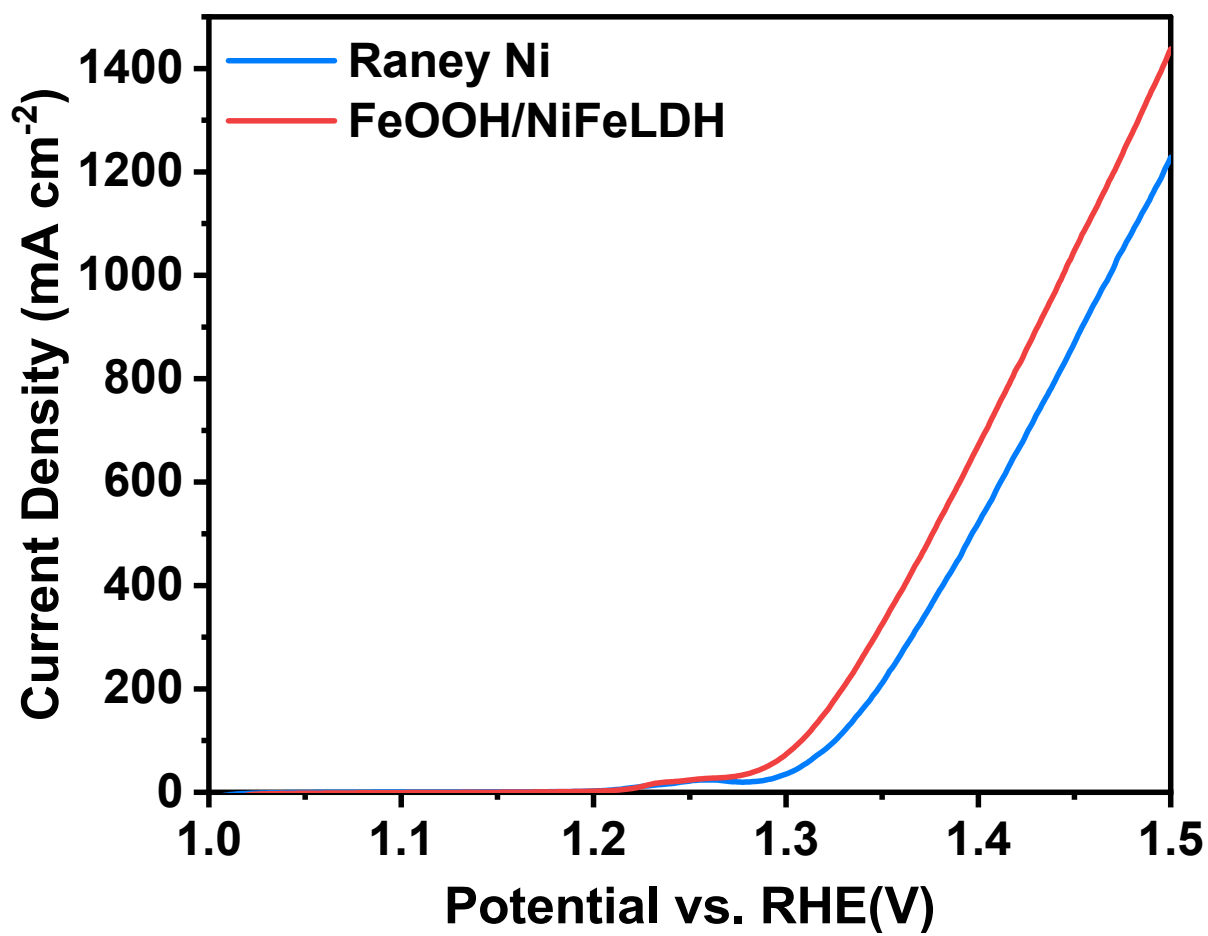
Fig. S17. OER polarization curves of FeOOH/NiFe-LDH and commercial Raney nickel.

Table S1. The fitting parameters for Nyquist plots of FeOOH/NiFe-LDH, NiFe-LDH, and IrO$_2$.

| Samples	R_s (Ω)	R_{bulk} (Ω)	CPE$_1$ Q_{bulk} ($\mu\Omega^{-1}$ s^n)	n_{bulk}	C_{bulk} (μF cm^{-2})	R_{ct} (Ω)	CPE$_2$ Q_{ct} ($\mu\Omega^{-1}$ s^n)	n_{ct}	C_{ct} (μF cm^{-2})
FeOOH/NiFe-LDH	1.10	0.10	0.96	0.50	84.24	0.50	0.85	0.86	610.59
NiFe-LDH	1.20	0.20	0.36	0.66	52.24	0.93	0.19	0.90	33.60
IrO$_2$	1.19	12.16	0.01	0.83	0.10	3.64	0.05	1.00	2.50

From CPE parameters (Q and n values, Q is the pre-factor of the CPE and n is exponent of the

CPE), the capacitance was calculated using equation of $C_{bulk/ct} = Q^{\frac{1}{n}}(\frac{1}{R_s} + \frac{1}{R_{bulk/ct}})^{\frac{\alpha-1}{\alpha}}$.[1]

Table S2. The binding energy (eV) for elements in FeOOH/NiFe-LDH and NiFe-LDH.

Samples	Ni 2p$_{2/3}$	Ni 2p$_{2/3}$ sat.	Fe 2p$_{2/3}$	O 1s Metal-O	O 1s Metal-OH	O 1s H$_2$O
FeOOH/NiFe-LDH	855.8	861.5	712.0	529.7	531.3	533.1
NiFe-LDH	855.6	861.3	712.4	529.6	531.3	533.1

Table S3. OER performance and synthesis details for typical NiFe-based catalysts.

Catalyst	Substrate	Method	Synthesis time	$\eta_{(100)}$ (mV)	Durability	Ref.
FeOOH/NiFe-LDH	NF[a)]	Fenton-like reaction	1 min	238	1.6 V, over 700 h	This work
FeOOH/Ni(OH)$_2$	NF	Electrodeposition and Electrophoretic deposition	>14 min	245*[b)]	40 mA cm^{-2}, 28 h	2
S-(Ni,Fe)OOH	NF	One pot solution-phase method	5 min	281	100 mA cm^{-2}, 100 h	3
Ni/NiFe(OH)$_x$	NF	Electrodeposition	2 s	290	100 mA cm^{-2}, 38 h	4
Ni–Fe–P	NF	Electroless deposition	1 h	290*	1.5 V, 8.3h	5
FeCoNiOOH	NF	Hydrothermal	6 h	330	100 mA cm^{-2}, 10 h	6
NiFeSe@Ni(Fe)OOH	NF	Hydrothermal and solution-phase reaction	>12 h	260*	100 mA cm^{-2}, 10 h	7
NiFe-LDH	CP[c)]	Two-step solution phase reaction	>7 h	280*	20 mA cm^{-2}, 50 h	8
Ni(OH)$_2$/FeOOH@NiFe	SSM[d)]	Sputtering-alloying-dealloying-activation	>6 h	260*	10 mA cm^{-2}, 1000 h	9
FeNiW-LDH	FF[e)]	Electrochemical corrosion	7 h	250*	300 mA cm^{-2}, 120 h	10
(Ni$_2$Co$_1$)Fe-MOF	GC[f)]	Solution-phase method	>1 h	310*	1.488 V, 35 h	11
FeCo-NiSe$_2$	CC[g)]	Hydrothermal and phosphorization	>7 h	360	10 mA cm^{-2}, 50 h	12
NiCe@NiFe/NF-N	NF	Two steps electrodepositing	>35 min	254	1000 mA cm^{-2}, 20 h	13
NiFe-LDH	CP	Coprecipitation	10 min	345*	10 mA cm^{-2}, 100 h	14
Fe$_{0.67}$Ni$_{0.33}$OOH-Fe$_2$O$_3$	NF	Hydrothermal	>65 min	310*	30 mA cm^{-2}, 110 h	15
NiFe@N-Carbon	CC	Hydrothermal and annealing	>14 h	263	20 mA cm^{-2}, 35 h	16
NiMoN@NiFeN	NF	Hydrothermal and thermal nitridation	>7 h	277	500 mA cm^{-2}, 48 h	17
FeOOH/LDH	GC	Hydrothermal	15 h	270*	10 mA cm^{-2}, 27 h	18

FeOOH@Ni(OH)$_2$	NF	Electrodeposition and alkali etching	> 4 h	280*	50 mA cm^{-2}, 40 h	[19]
FeOOH@Ni(OH)$_2$	GC	Hydrothermal	> 26 h	430*	10 mA cm^{-2}, 12 h	[20]
Fe-β-Ni(OH)$_2$	NF	Hydrothermal	5 h	280*	-	[21]

[a])(NF: Ni foam); [b])(*: Value calculated from curves shown in the respective reference.); [c])(SSM: stainless steel 410); [d])(SSM: stainless steel 410); [e])(FF: Fe foam); [f])(GC: glassy carbon); [g])(CC: carbon cloth);

References

1   B. Hirschorn, M. E. Orazem, B. Tribollet, V. Vivier, I. Frateur and M. Musiani, *Electrochim. Acta*, 2010, **55**, 6218-6227.

2   S. Niu, Y. Sun, G. Sun, D. Rakov, Y. Li, Y. Ma, J. Chu and P. Xu, *ACS Appl. Energ. Mater.*, 2019, **2**, 3927-3935.

3   X. Chen, Y. Meng, T. Gao, J. Zhang, X. Li, H. Yuan and D. Xiao, *Sustain. Energ. Fuels.*, 2020, **4**, 331-336.

4   S. Zhuang, L. Wang, H. Hu, Y. Tang, Y. Chen, Y. Sun, H. Mo, P. Wan and Z. U. H. Khan, *ChemElectroChem*, 2018, **5**.

5   K. Wang, K. Sun, T. Yu, X. Liu, G. Wang, L. Jiang and G. Xie, *J. Mater. Chem. A*, 2019, **7**, 2518-2523.

6   Q. Zhang, N. M. Bedford, J. Pan, X. Lu and R. Amal, *Adv. Energy Mater.*, 2019, **9**, 1901312.

7   Y. X. Li, D. F. Yan, Y. Q. Zou, C. Xie, Y. Y. Wang, Y. Q. Zhang and S. Y. Wang, *J. Mater. Chem. A*, 2017, **5**, 25494-25500.

8   J. Zhang, L. Yu, Y. Chen, X. F. Lu, S. Gao and X. W. Lou, *Adv. Mater.*, 2020, **32**, 1906432.

9   J. Zhang, Y. Bai, C. Zhang, H. Gao, J. Niu, Y. Shi, Y. Zhang, M. Song and Z. Zhang, *ACS Sustain. Chem. Eng.*, 2019, **7**, 14601-14610.

10   J. He, X. Zhou, P. Xu and J. Sun, *Nano Energy*, 2021, **80**, 105540.

11   Q. Qian, Y. Li, Y. Liu, L. Yu and G. Zhang, *Adv. Mater.*, 2019, **31**, 1901139.

12   Y. Sun, K. Xu, Z. Wei, H. Li, T. Zhang, X. Li, W. Cai, J. Ma, H. J. Fan and Y. Li, *Adv. Mater.*, 2018, **30**, 1802121.

13   G. Liu, M. Wang, Y. Wu, N. Li, F. Zhao, Q. Zhao and J. Li, *Appl. Catal. B: Environ.*, 2020, **260**, 118199.

14   X. Zhang, Y. Zhao, Y. Zhao, R. Shi, G. I. N. Waterhouse and T. Zhang, *Adv. Energy Mater.*, 2019, **9**, 1900881.

15   M. Wang, K. Cao, Z. Tian and P. Sheng, *Appl. Surf. Sci.*, 2019, **493**, 351-358.

16   C. Wang, H. Yang, Y. Zhang and Q. Wang, *Angew. Chem. Int. Edit.*, 2019, **58**, 6099-6103.

17   L. Yu, Q. Zhu, S. Song, B. McElhenny, D. Wang, C. Wu, Z. Qin, J. Bao, Y. Yu, S. Chen and Z. Ren, *Nat. Commun.*, 2019, **10**, 5106.

18   J. Chen, F. Zheng, S.-J. Zhang, A. Fisher, Y. Zhou, Z. Wang, Y. Li, B.-B. Xu, J.-T. Li and S.-G. Sun, *ACS Catal.*, 2018, **8**, 11342-11351.

19   W. Guo, D. Li, D. Zhong, S. Chen, G. Hao, G. Liu, J. Li and Q. Zhao, *Nanoscale*, 2020, **12**, 983-990.

20   J. Wang, S. Li, R. Lin, G. Tu, J. Wang and Z. Li, *Electrochim. Acta*, 2019, **301**, 258-266.

21   T. Kou, S. Wang, J. L. Hauser, M. Chen, S. R. J. Oliver, Y. Ye, J. Guo and Y. Li, *ACS Energy Lett.*, 2019, **4**, 622-628.